Modelling the spatiotemporal change of canopy urban heat islands

Jasim M. Ali [a,b] , Stuart H. Marsh [a] , Martin J. Smith[a]

[a] Faculty of Engineering, The University of Nottingham, Nottingham, UK

[b] Faculty of Engineering, University of Anbar, Anbar, Iraq

Corresponding author : Jasim Ali

Email: Jasima094@gmail.com

Mobile: 07462271171

Abstract

This study models the spatiotemporal change of Birmingham's urban heat island (UHI) using air temperature measurements made during the HiTemp project to study the atmospheric conditions over the city [1]. The study identifies the causative factors and their contributions to the formation of UHI, based on a number of data used to build 2.5 D model; land cover, land use, geometrical factors and shadow layers. The raw air temperature measurements were filtered, georeferenced and interpolated to create maps of temperature variations. The expected influencing parameters on the development of the UHI were derived and prepared for regression modelling. The results showed that the difference in temperature across Birmingham city through two years of ground measurements (June 2012 – June 2014) reached up to 13.53 °C. The UHI's appeared daytime and night-time throughout the different seasons for approximately 56% of the total hours during the study period. However, the high intensity events happened during the calm and clear nights. Moreover, buildings' shadow provided up to 2 °C reduction to the air temperature, while the wind speed and direction are responsible for the size and distribution of hot spots. The built up area contributed to increase the UHI, whereas, the other types of land cover and the geometrical parameters, contributed less.

Keywords: urban heat island, high resolution measurements, spatiotemporal change, influencing parameters, regression models

1- Introduction

The phenomenon of heat islands was first documented in 1818, when Luke Howard found an artificial excess of heat in the city centre of London compared to the surrounding country [2]. This excessive heat has been long observed in urban and suburban areas where air and surface temperature are higher than their adjacent rural areas. The traditional way of measuring the Urban Heat Island (UHI) is by measuring the air temperature using a pair of meteorological stations to calculate the Atmospheric Urban Heat Island (AUHI). Remote sensing (RS) techniques can capture the surface temperature as an indicator of the so called Surface Urban Heat Island (SUHI) [3]. The increase in availability of high spatial resolution satellite images has enabled researchers to study the spatial change of surface temperature patterns, but it does not always capture the temporal variation of heat islands [4, 5]. The heat islands have been classified based on different attributes. Cermak, et al. [6] classified the urban climate into three layers, the first layer describes a street and its surrounding buildings, which is called the canyon layer. Second, the canopy layer extends upwards from the surface to approximately mean building height. Third, the boundary layer is a layer of air up to 2000 meters height above the canopy layer. Voogt and Oke [7] explained that there are three types of UHI. The surface heat island refers to the difference in surface temperature between the urban and rural areas. The canopy heat island indicates the difference in air temperature between urban and rural areas within the canopy layer. The boundary heat island measures the difference in air temperature between the urban and rural areas within the boundary layer. AUHI and SUHI have different spatiotemporal behaviour, and they are two different approaches to study the UHI phenomenon [8]. While, the expensive approach of RS is focused on the SUHI that lacks the temporal resolution; the AUHI employs the field measurements which usually have limited spatial resolution due to limited stationary network or mobile stations around a city [9]. This paper adopts a dense network of meteorological sensors to provide high spatial resolution as well as high temporal resolution of AUHI measurements within the canopy layer.

Environmental Protection Agency (EPA) [10] explained that the factors that might create UHIs include: reduced vegetation in urban areas, the thermal properties of urban material, urban geometry, anthropogenic heat emissions, weather, and topography. Some of these factors are natural occurrences and engineers cannot control them such as weather and geographic location. However, some other factors can be changed by design, such as the properties of building materials. The negative consequences of UHI include increased energy consumption, greenhouse gases, human discomfort, and impaired water quality [11]. Mirzaei, et al. [12] explained that increased peak demand, mortality, and morbidity are the most important negative consequences of UHI. Indeed, whilst some communities might benefit from the excessive heat in winter in terms of energy consumption, the summer penalty is much larger and it can affect a community's environment and quality of life [10]. Sailor [13] explained that the canopy UHI is most relevant with respect to direct effects on building occupants, particularly in the summertime, buildings located in or near the centre of a large city tend to have the largest energy consumption in the early morning hours. Conversely, Berger, et al. [14] in their study concluded that hottest locations in moderate climates tend to reduce energy demands in the wintertime. From that, the identification of UHI events in terms of location, time and magnitude would help building designers for the more accurate simulation of building energy usage particularly for air conditioning and refrigeration [14]. So, urban planners should take into account the impacts of UHI for future cities, and work on the possible solutions to mitigate theme in existing cities.

The recent AUHI studies within the canopy layer presented in the literature have not used high spatial and temporal resolution temperature together. Furthermore, they have not modelled all the important controllable factors that potentially affect the development of UHI. For example, Busato, et al. [15] have reported their experimental results for three years of mobile traverses, which covered prefixed paths in the city of Padua in Italy. However, this traversing approach does not fully explain the impacts of topography and the effects of different land covers. Doick, et al. [16] investigated the impact of Kensington Gardens a park land area in London, and the findings showed the importance of vegetation in UHI mitigation. Nevertheless, the study also revealed the uncertainty over the variables that govern the extent of UHI. This result supports Ivajnšič, et al. [17] who they concluded that local and regional variables have a very important role in explaining spatial variation in mean air temperature. Whilst, large scale studies of UHI have been based mainly on remotely sensed satellite images, they have lack the temporal variation of real time land surface temperature [18-21]. A study by Ho, et al. [22] assessed the ability of three remote sensing-based regression models to map the peak daytime air temperature used a dense observation weather stations. However, this study was very limited temporarily as it used only six satellite images and focused on extreme events of air temperature. To address this deficiency, a novel project called HiTemp has been undertaken by The Birmingham Urban Climate Laboratory (BUCL) funded by The Natural Environment Research Council (NERC) [1]. It has provided near real time data from one of the densest urban meteorological network of automatic weather stations worldwide [23]. This project is ongoing since June 2012, and covers the entire conurbation of Birmingham.

The aim of this research is to model the spatial and temporal variation of UHI using a dense network of meteorological sensors, and to investigate the influence of a number of important influencing parameters on the AUHI formation. Accordingly, the major objectives of the research are divided into three themes time, location and parameters. The temporal resolution of the data starts from hourly basis to monthly time increment, whereas, the spatial resolution relies on the distribution of HiTemp stations' locations. The influencing parameters are grouped into land cover/land use, geometrical and meteorological factors and these parameters will be tested to investigate their impact on the UHI.

2- Methodology

A. Study area

Birmingham is the largest populated local authority in the UK, with 1,101,400 persons based on the annual mid-year population estimate in a 2014 report published by the office for National Statistics [24]. Its conurbation extends to around 2778 square kilometers over the West Midland [25]. Tomlinson, et al. [25] highlighted that the city used to have only one weather station for urban areas and another station outside the city in the rural areas. The UHI studies on Birmingham are very few in relation to its size and importance. Unwin [26] did one of the earliest studies about Birmingham UHI by comparing the temperature measurements between a site in the city and a rural area. A maximum of 5 ºC UHI intensity was observed in settled anticyclonic conditions. Similarly, Johnson [27] found a maximum of 4.5 ºC UHI intensity using a mobile traverse technique. After that, Bradley, et al. [28] used a 1-dimesional energy balance model to capture a maximum of 4.7 ºC SUHI. Recently, Tomlinson, et al. [25] identified a maximum of 5 ºC in the central business district during high atmospheric pressure periods, and also recorded cold spots in one park of up to 7 ºC lower than the city centre. So, Birmingham was considered a good site to investigate the effects on UHI's.

B. Data

The air temperature data from the HiTemp project was provided by NERC for the purposes of this study. The temperature readings consist of two main types of sensors: over 80 wireless Aginova Sentinel Micro (ASM) sensors record only air temperature, while 25 Automatic Weather Stations (AWS) record the main meteorological variables [23]. All these stations capture the meteorological data per minute, and the data obtained for this study is from June 2012 to June 2014. Fig.1 shows the HiTemp distribution of stations inside the boundary of the city, and the station locations were obtained from the Meta data of the project. AWS and ASM are denoted with the prefix W and S respectively as shown in Fig.1. Schools were selected to host the majority of sensors as they are relatively secure and representative of their local environment [23]. Also, Birmingham's schools have a good coverage of the city, and mostly connected to Wi-Fi networks for data transmission. Furthermore, the points for sensors installed more than 20 m away from heat sources, and the ASM sensors have approximately 3 km average spacing [23]. ASM provide only temperature data, however AWS give other meteorological data such as wind speed and direction which will be considered alongside the analysis of the temperature data [1].

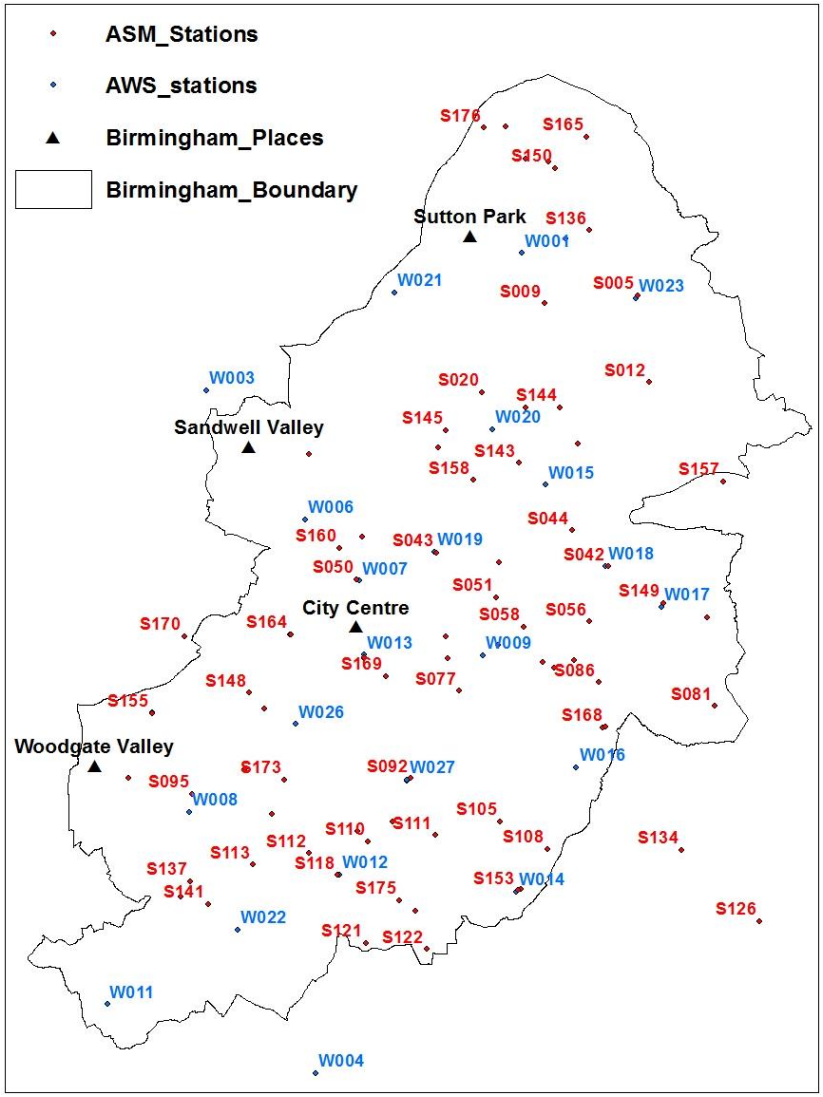

Fig. 1 HiTemp Station locations in Birmingham

The air temperature is used as an indicator of UHI, and it is the dependent variable that will be analysed and investigated against the predictor variables of the influencing parameters. The influencing parameters on the formation of UHI that are used in this study can be grouped into three main categories: land cover/land use, urban geometry and meteorology. There are other influencing parameters not modelled in this study such as the radiation fluxes and anthropogenic activities will be investigated in future work.

i. Land cover/land use

Four land cover/land use data sets of Birmingham city have been used to capture all the variations of the physical environment such as buildings, pavements, parks and water. The first set of urban data is the Ordnance Survey (OS) Master Map Topography Layer which contains information about the objects on the ground divided into themes and descriptive groups [29]. The version of the OS vector data updated in June 2015 has been used as it includes data stored in geodatabases useful for GIS urban mapping as detailed in Fig.2 and Fig.3. The descriptive groups are more detailed collections of the generalised themes, and it is feasible to examine the influence of both. A descriptive group is the primary classification attribute of a feature, which assigns a feature to one or more of 21 groups [30]. Whilst, a theme is a set of features that have been grouped together for the convenience of customers and to provide a high-level means of dividing the data on the layer coherently or logically. As a result, one classification might be more sensitive to air temperature change than the other.

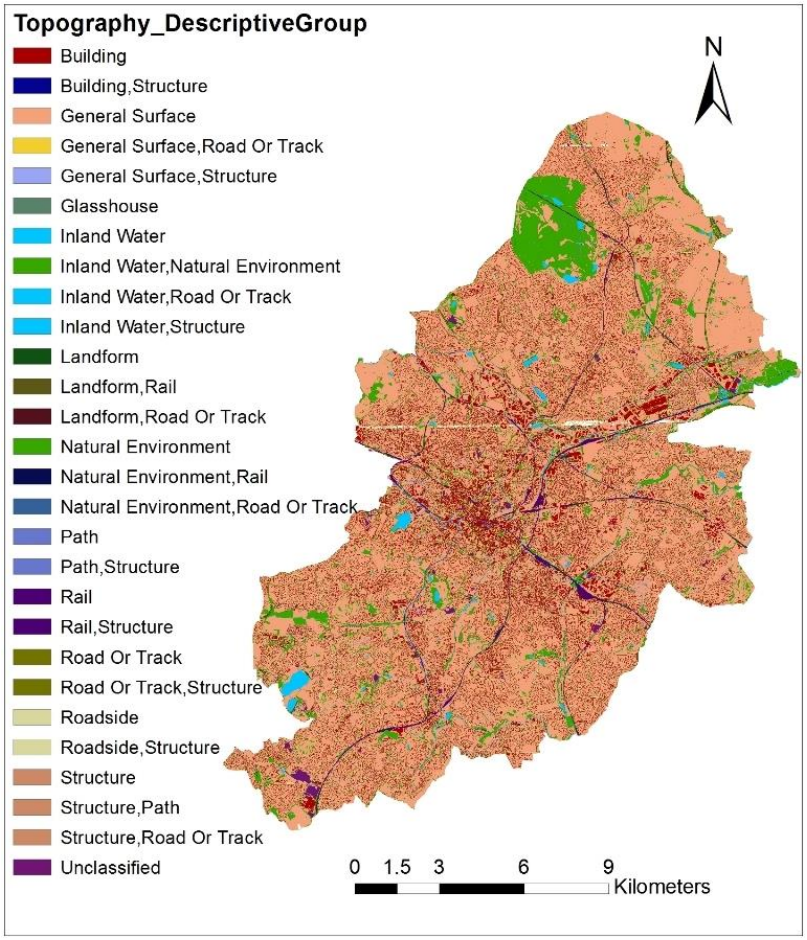

Fig. 2 Descriptive group of topography layer adopted from [20]

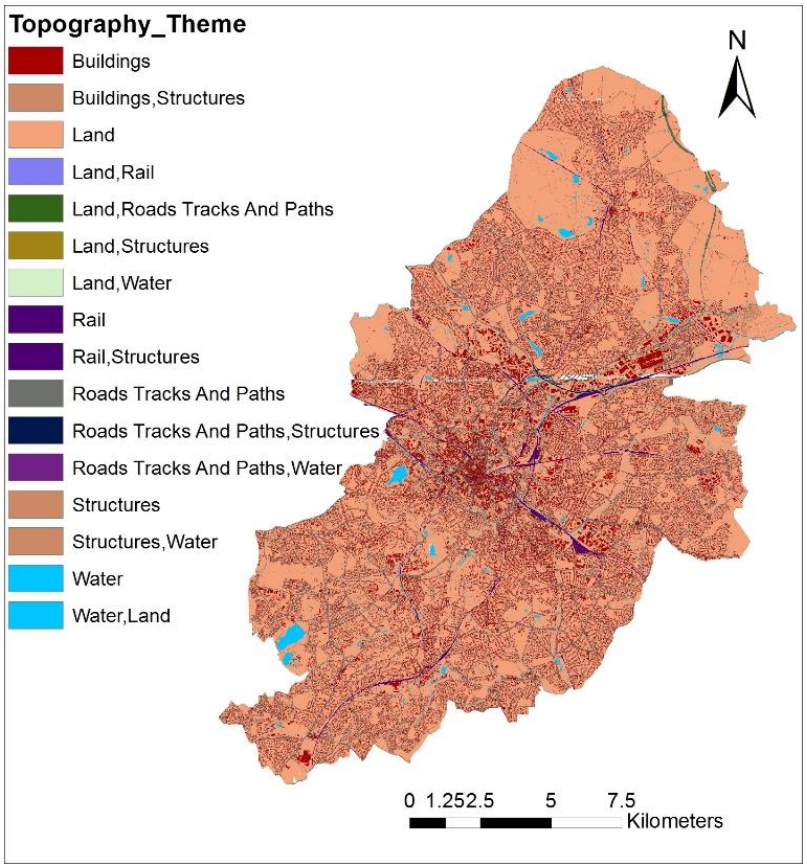

Fig. 3 Themes of topography layer adopted from [20]

The second set of data is the land use map including low density urban fabric classified by the European Environment Agency based on SPOT 5 images (2010) and city map (2008). These high resolution classes as shown in Fig.4 were downloaded from the European Urban Atlas and it is available for large urban zones with more than 100000 inhabitants as defined by the Urban Audit [31].

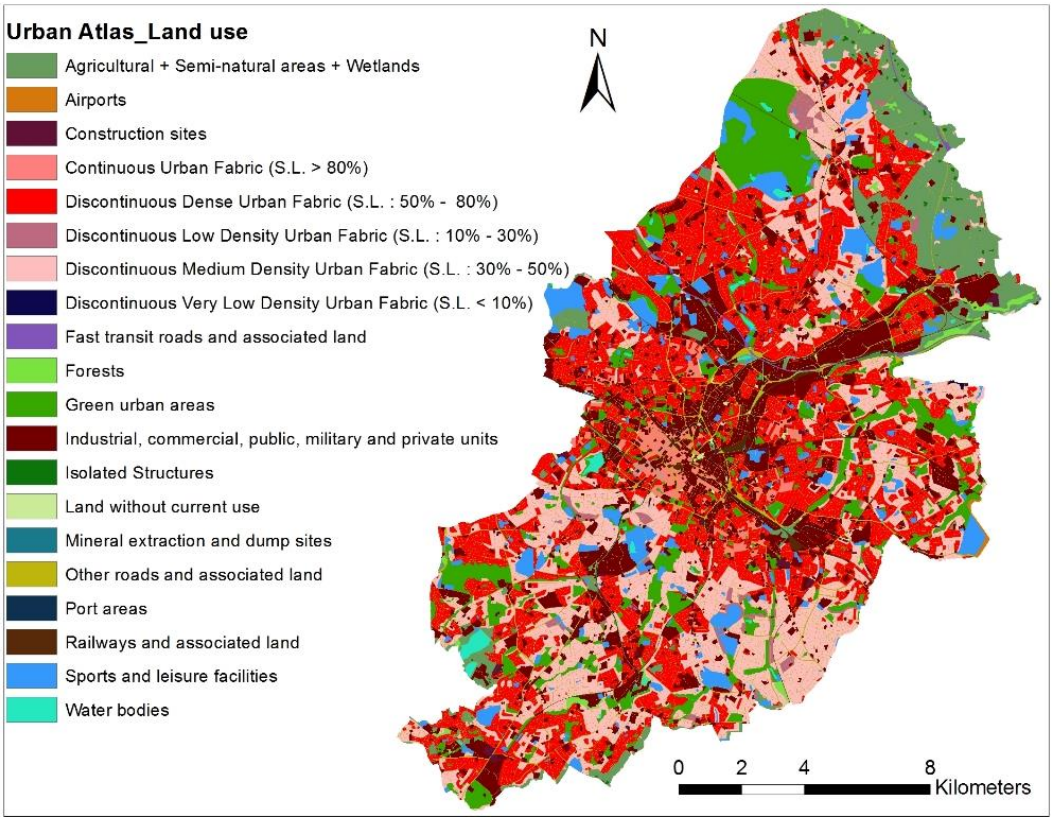

Fig.4 Urban Atlas of land use adopted from [21]

The third set of data classifies the differing urban land use to eight categories, and it splits the urban fabric into multiple categories allowing more in depth comparison [25]. It uses data from OS and the UK Center for Ecology and Hydrology (CEH) classified by a principle component analysis and cluster analysis [32]. The classification scheme was based on 27 different input attributes and the output spatial resolution is a 1 km^2 grid showing similar urban land morphology (for more details see [32]). The result map of this approach is shown in Fig.5, which consists of eight categories urban land use classification derived per pixel based on their common land use. It can be seen that they city centre is classified as urban or transport, and most of the villages and farms are close to the city's boundary.

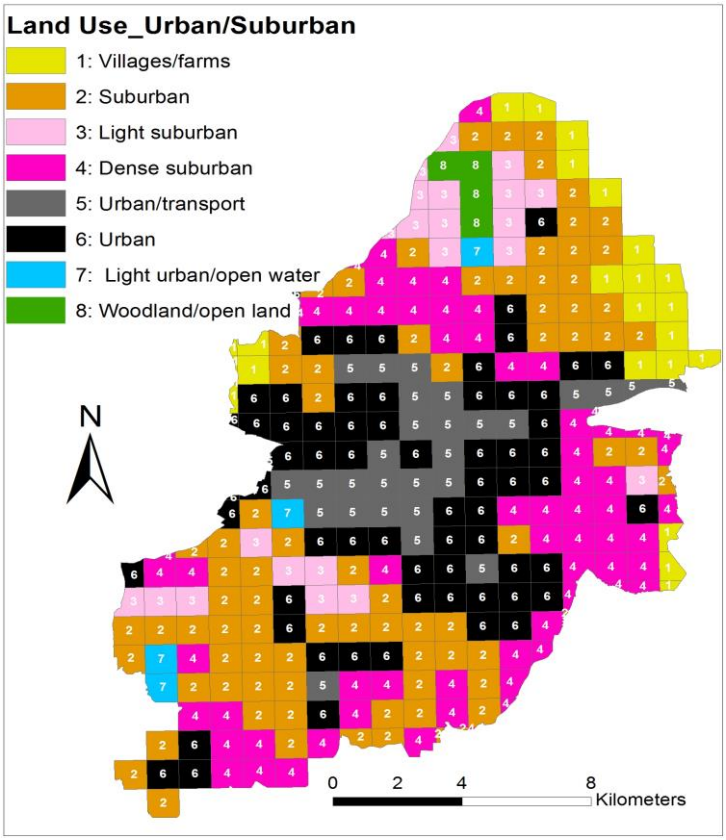

Fig. 5 Spatial distribution of land classification[25]

The fourth data set is high resolution raster images (25 cm) obtained from the Ordnance Survey based on a licensed agreement for the purpose of this study [33]. This dataset is employed to georeference other data layers and interpret the classification of the mentioned land cover/land use maps with the help of the ArcGIS online basemap. These basemaps and reference layers are freely available to anyone and include World Imagery, World Street Map, World Topographic, Ocean Basemap, and more [34]. Fig.6 gives an example of images of locations identified in Fig.1 using the high resolution OS images.

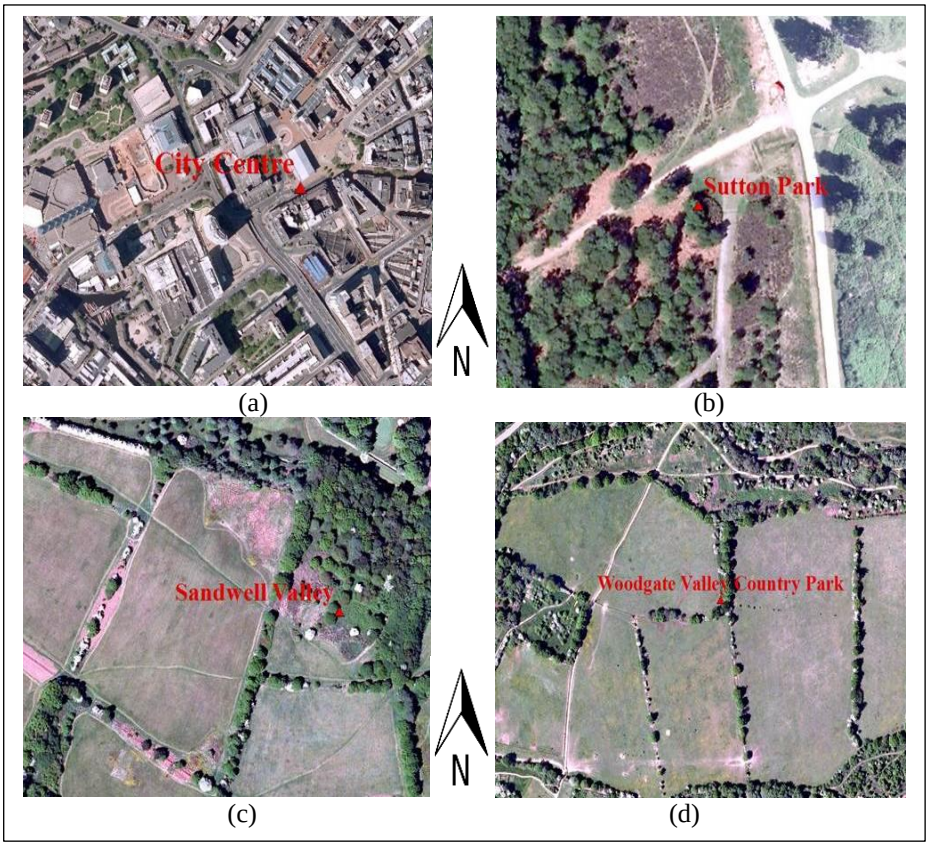

Fig. 6 OS high resolution maps (a) City Centre, (b) Sutton Park, (c) Sandwell Valley and (d) Woodgate Valley Country Park at 1:2500 scales

ii. Urban Geometry

Two digital elevation models were prepared to derive the geometrical factors (such as sky view factor and shadow patterns); the Digital Surface Model (DSM) and Digital Terrain Model (DTM) as shown in Fig.7. The 1m resolution DSM is obtained from the UK Environment Agency free of charge for academic purposes. It provides height data of buildings and other features on the ground using airborne LiDAR technology [35]. On the other hand, OS Terrain 5 DTM is a 5 m resolution product captured as a triangulated irregular network (TIN), which is a three dimensional model edited to exclude buildings, trees and other above ground features created within a photogrammetric environment [30].

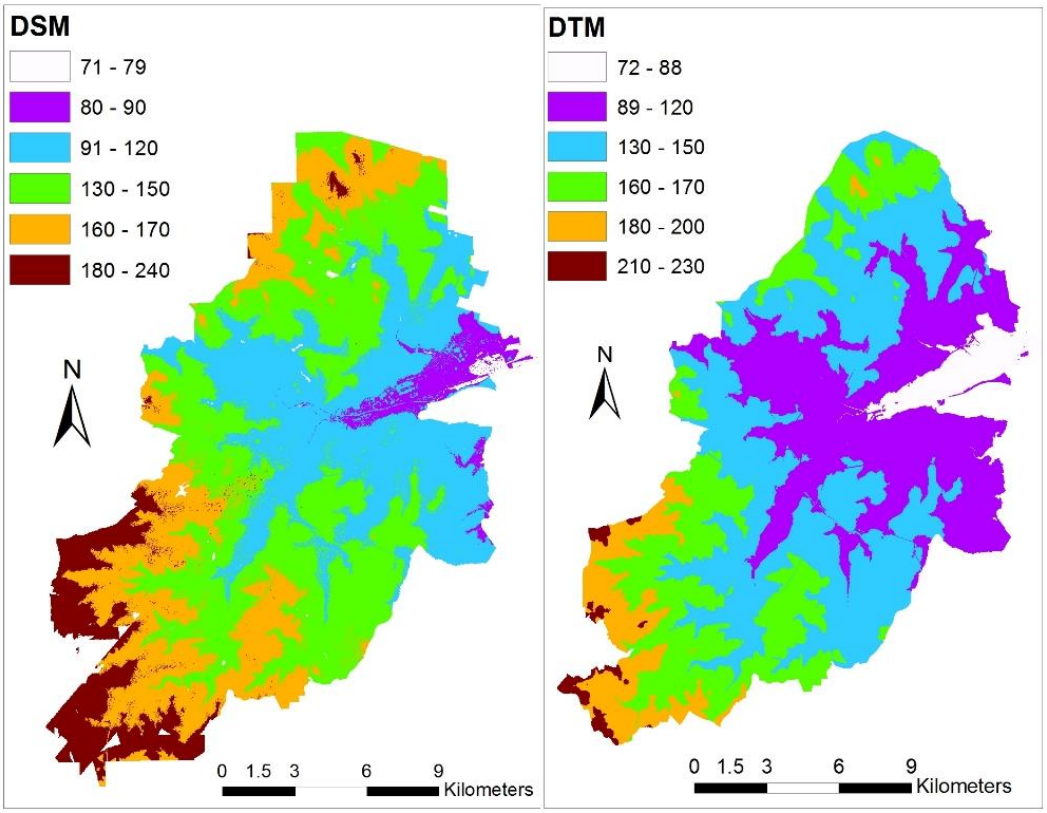

Fig. 6 DSM and DTM models (meters)

iii. Meteorological data

The hourly meteorological variables not available from the HiTemp have been acquired from The Centre for Environmental Data Archival (CEDA). CEDA is a data center for the atmospheric sciences run by the Natural Environment Research Council (NERC). Rainfall, cloud cover, solar radiation and soil temperature data for ground stations in Birmingham were downloaded from the Met office Integrated Data Archive System (MIDAS) catalogue [36].

C. Method

Most of the input data required format conversion, extent extraction and resampling to be handled and overlaid with other layers in ArcGIS and other software. GIS applications have been commonly used to represent the current status and plan the future of the urban environment, as they are well suited to address spatial data and visualization issues associated with multiscale geographical data [37]. Wong, et al. [38] employed the integration of GIS, GPS and logging sensors in microclimate monitoring to study impact of environmental and human factors on urban heat in

Hong Kong. Furthermore, ArcGIS and ENVI were coupled to investigate and identify land use types which had the most influence to the increase of ambient temperature in Singapore [39].

Initially, the air temperature data is a raw data divided into daily files for individual stations. Erroneous readings were identified from flags assigned to each observation provided by the BUCL guide, and omitted. Temperature records were extracted from each station for a specific time with the coordinates and elevation. These text files were exported to ArcGIS to be converted to feature class and raster images by Inverse Distance Weighting (IDW). A statistical and spatial analysis was then performed to find the high intensity urban heat island hours. The hourly time scale is sufficient for the purpose of this study, and any unexpected values were investigated.

The land cover data was extracted to the extent of the study site after converting its format to raster images. Also, a data extractor tool called CEDA Web Processing Service (WPS) was used to extract the meteorological data from MIDAS for the time period and spatial range of the study. The high resolution DSM model and OS Mastermap was built by mosaicking the 1 square kilometre grids and converting the formats to raster images.

The next stage is processing and modelling the influencing parameters. Land cover data was extracted to include all the various physical parameters. Then, geometrical factors such as Sky View Factor (SVF), visible sky and terrain view factor were derived using the DSM as input to the free and open source Quantum GIS (QGIS). Shadow patterns and illumination images were constructed for the days of high UHI intensity. The last stage of the method is building multiple linear regressions, where the relationship between air temperature and the variables (influencing parameters) can be explored. After building and running the regression models using Microsoft Excel, the models are enhanced using backward elimination method until a significant model was found. The backward elimination method is an economical procedure to choose the best regression equation by removing the variable being investigated that has the highest P value until the model becomes significant [40]. The P value (or the observed significance level) is the smallest fixed level at which the null hypothesis can be rejected [41]. A variable is considered significant if its p-value is less than 0.05 at a confidence level 95%, and the relationship becomes highly significant if the p-value is less than 0.01.

3- Results and discussion

A- UHI temporal change

The historical air temperature data (1990-2014) for the city centre of Birmingham was acquired from the Met Office [36] for the purpose of validating the use of HiTemp data from June 2012- June 2014. Fig.8 draws the averages of the maximum and minimum air temperatures with their trends for the period (1990-2014). The mean of the maximum and minimum for the 25 years was 13.01 and 6.91, respectively, with standard deviations of 0.75 (maximum) and 0.77 (minimum). The means of the maximum temperature for the 2012-2014 years were 12.83, 12.40 and 13.30, and for the minimum were 6.36, 6.96 and 7.52 respectively (all temperatures in ^{o}C). The averages of the temperatures during the period 2012-2014 lie within the mean and the standard deviation of the 25 years historical data. So, this 2 years (HiTemp Project) period can be considered typical for the period covered by the historical data. However, the averages of the maximum and minimum air temperatures during the period (2012-2014) for the collected data are 12.19 and 9.68 with standard deviations 5.30 and 5.72 respectively.

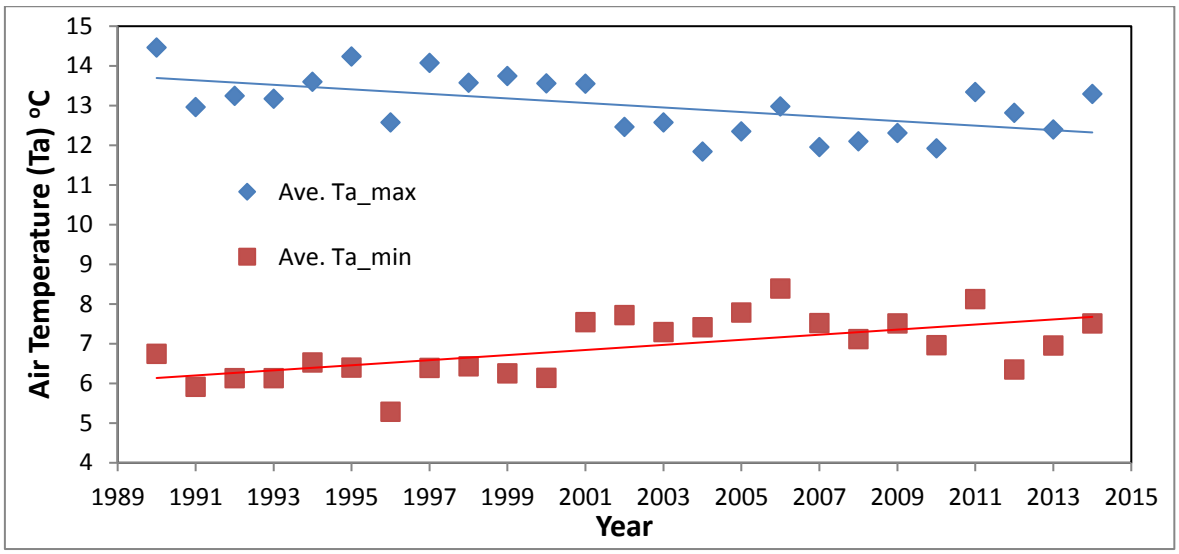

Fig. 7 Historical air temperature of Birmingham City

The data was analysed per hour to summarise the variation of UHI, then monthly statistics were calculated to show the seasonal change of temperature patterns. Also, extreme events were identified with the climatic condition and hot spots' spatial distribution was conducted. The hourly statistical analysis of UHI for 2 years of measurements has demonstrated that around 56% of total 17520 hours gave an air temperature variation more than 1.5 °C in the city of Birmingham. This was used to set a threshold of 1.5 ºC difference in temperature as a minimum variation to indicate the UHI's presence. Interestingly, the highest UHI intensity was in September, at 13.5 °C, and the lowest intensity 5 °C was in January. However, the highest average temperature 3.9 °C was monitored in July, whereas, the lowest average was in January by 2.3 °C. Besides, the longest hours of occurrence of an UHI were in June by 1323 hours, and the shortest, 471 hours of occurrence were in February.

Table 1 Statistical summary of UHI analysis

Statistics\Month	Dec.	Nov.	Oct.	Sep.	Aug.	Jul.	Jun.	May	Apr.	Mar.	Feb.	Jan.
Count(hr)	719	853	715	806	727	686	1323	1184	1104	854	471	476
Ave. UHI (°C)	2.5	2.6	2.5	3.5	3.3	3.9	3	3	2.8	2.8	2.4	2.3
Max. UHI (°C)	9.1	6.3	6.8	13.5	7.6	13.4	9.6	10.7	7.9	12.4	6.7	5

Moreover, UHI events with intensity over 10 °C showed that it can happen in the evening, night or early morning times as detailed in Table 2. Table 2 includes the date and time of the highest UHI events over 10 °C with the averages of wind speed, also the times of sunrise and sunset were added to distinguish between the day and night [42]. The extreme events (over 10 °C) are listed in table 2 in descending order, regardless, of the dates of occurrence, to show their magnitude and time. It is important to notice that none of the highest intensity UHI (over 10 °C) coincided with the heat wave that affected most of the UK from 3 to 23 July 2013. This might be due to the local instant effect of UHI, while, the heat waves have larger regional influence. The UHI induces more intense heat waves through the global warming in the long term, and the former is being referred to as either a cause or consequence of the later [43]. Met office has declared the July 2013 heat wave as the third warmest on record, and this month as the warmest and sunniest for the whole UK since 2006 [44]. Nevertheless, the highest temperature in 2013 recorded by the Met Office stations in Birmingham was 30.5 °C on the 1 August 2013 at 3pm [36], while, using HiTemp network the temperature in Birmingham at the same time was 31.2 °C. Furthermore, it was not the highest temperature recorded by HiTemp on that day, as it recorded 32.34 °C on the same day (1 August 2013) at 5pm. This difference between Met Office and

HiTemp' readings might be due to the height of the sensors. HiTemp sensors were installed at 3 m (with exceptions no more than 0.5m higher or lower), though, Met Office sensors almost installed 5 m above the ground level [23]. This makes the 3m high sensors be more affected by surrounding surface heat, as they are closer to the energy sources [23]. Furthermore, the Met Office stations do not cover the full variation of the temperature due to the limited number of stations. On the other hand, most of the extreme events in table 2 coincided with calm (< 1 m/s) or light air (1-2 m/s) wind speed as described by the Beaufort wind force scale [45]. This agrees with Roth [46] that the heat island is greatest under light wind conditions.

Table 2 UHI intensity over 10 °C events and average wind speed

Date	Hour	Sunrise	Sunset	UHI Intensity	Ave. Wind Speed (m/sec.)
04/09/2013	19	06:25	19:47	13.53	0.44
05/09/2013	17	06:26	19:45	13.46	1.52
01/07/2013	21	04:50	21:33	13.37	0.53
01/07/2013	20	04:50	21:33	13.22	0.88
01/07/2013	22	04:50	21:33	13.17	0.54
05/09/2013	18	06:26	19:45	12.74	2.04
04/09/2013	20	06:25	19:47	11.83	0.39
04/09/2013	18	06:25	19:47	11.68	0.92
03/09/2013	19	06:23	19:49	11.60	0.36
07/09/2013	18	06:30	19:40	11.56	1.13
03/09/2013	18	06:23	19:49	11.27	0.53
01/07/2013	19	04:50	21:33	11.26	1.31
01/07/2013	16	04:50	21:33	11.20	1.85
05/09/2013	19	06:26	19:45	11.04	2.13
04/09/2013	21	06:25	19:47	11.02	0.31
05/09/2013	05	06:26	19:45	10.72	0.40
05/09/2013	01	06:26	19:45	10.70	0.62
24/05/2013	11	04:57	21:11	10.67	2.31
01/07/2013	17	04:50	21:33	10.64	1.85
05/09/2013	04	06:26	19:45	10.63	0.36
05/09/2013	03	06:26	19:45	10.60	0.47
05/09/2013	02	06:26	19:45	10.56	0.47
01/07/2013	18	04:50	21:33	10.45	1.84
04/09/2013	17	06:25	19:47	10.38	0.97
04/09/2013	22	06:25	19:47	10.33	0.45
05/09/2013	00	06:26	19:45	10.25	0.67
16/09/2013	17	06:45	19:19	10.18	2.33
05/09/2013	06	06:26	19:45	10.18	0.67
04/09/2013	23	06:25	19:47	10.01	0.43

B- UHI spatial change

The UHI was found to be concentrated in the city centre when its intensity was close to the mean values, however the extreme intensities were seen to stretch to the suburban areas due to the weather parameters in particular, the wind. Oke [47] stated that the maximum atmospheric UHI develops 3-5 hours after the sunset in clear and calm weather. The analysis of HiTemp data supported Oke's [47] claim, however, high intensity UHI can happen in the early morning, before sunset, or during the day in a cloudy weather when not much of the sun's radiation reaches the ground to change the surface energy balance. Fig. 9 gives examples of strong UHI's at the city centre for each season, and the layer name in the legend provides the date and time of the image in the format of year, month, day and hour. It can be seen that the highest intensities of UHI appear in or around the city centre, and the size of the red spot reveals the extent of the coverage. However, there are some spots of high intensity UHI away from the city centre; this is mainly due to the wind speed and direction as shown in Fig.10. Furthermore, the coldest spots clearly appear in the Sutton

Park which is the largest park in Birmingham that has vegetation and trees. Fig.10 shows the wind speed and direction for the same dates and time as Fig.9, and it can be seen that on average for the entire Birmingham area the low wind speed coincides with high UHI intensity. Wind speed is relatively high when the hot spots are concentrated in and around the city centre, because the presence of high buildings traps the release of heat into the atmosphere and increases the speed of the air flow. Whilst, the wind direction does not impact on the UHI intensity, it affects the size and distribution of the hot and cold spots. So, the UHI intensity is high for different wind directions, however, the size and distribution of hot spots are fluctuated for the dates and times in Fig.10 especially for (2013_9_5_7). With high wind speeds outside the city and its patterns change in direction around the city, to create sparse hot spots in the city and away from it. To investigate the daily change of UHI, Fig.11 shows the movement of hot and cold spots over the city in different times for a selected day where the UHI intensities are close to the average, detailed in table 1. The heat islands concentrate in and around the city centre during the night and early morning, and then move clockwise to Sutton Park to return to the city centre after sunset. Sunrise and sunset on the 6 October 2013 were 4:53 and 21:31 respectively [42], with average wind speed 1.33 m/s. It can be seen that when Sutton Park becomes a heat island, the city centre works as a cool island compared with their adjacent areas. Other influencing parameters on the formation of UHI will be investigated later in this study.

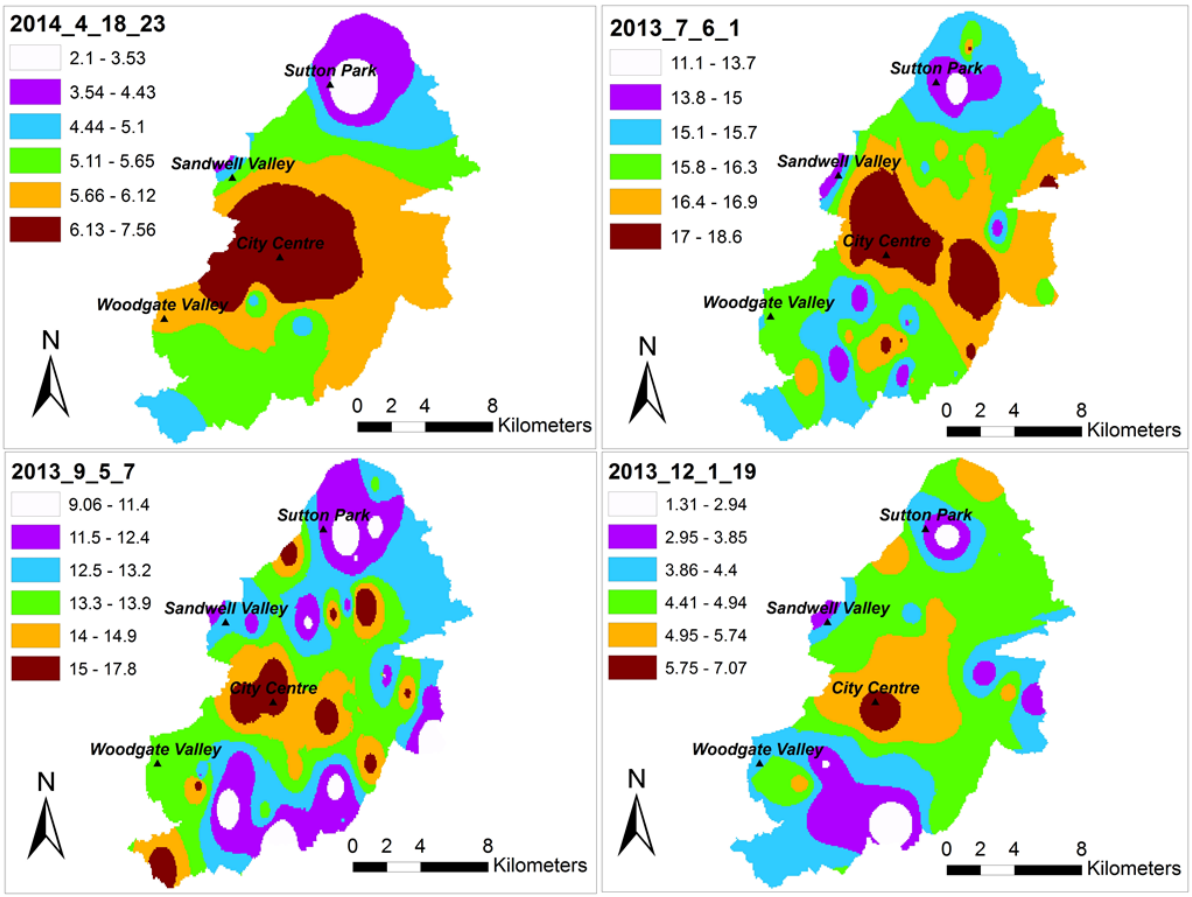

Fig.8 Seasonal UHI distribution in Birmingham (^{O}C)

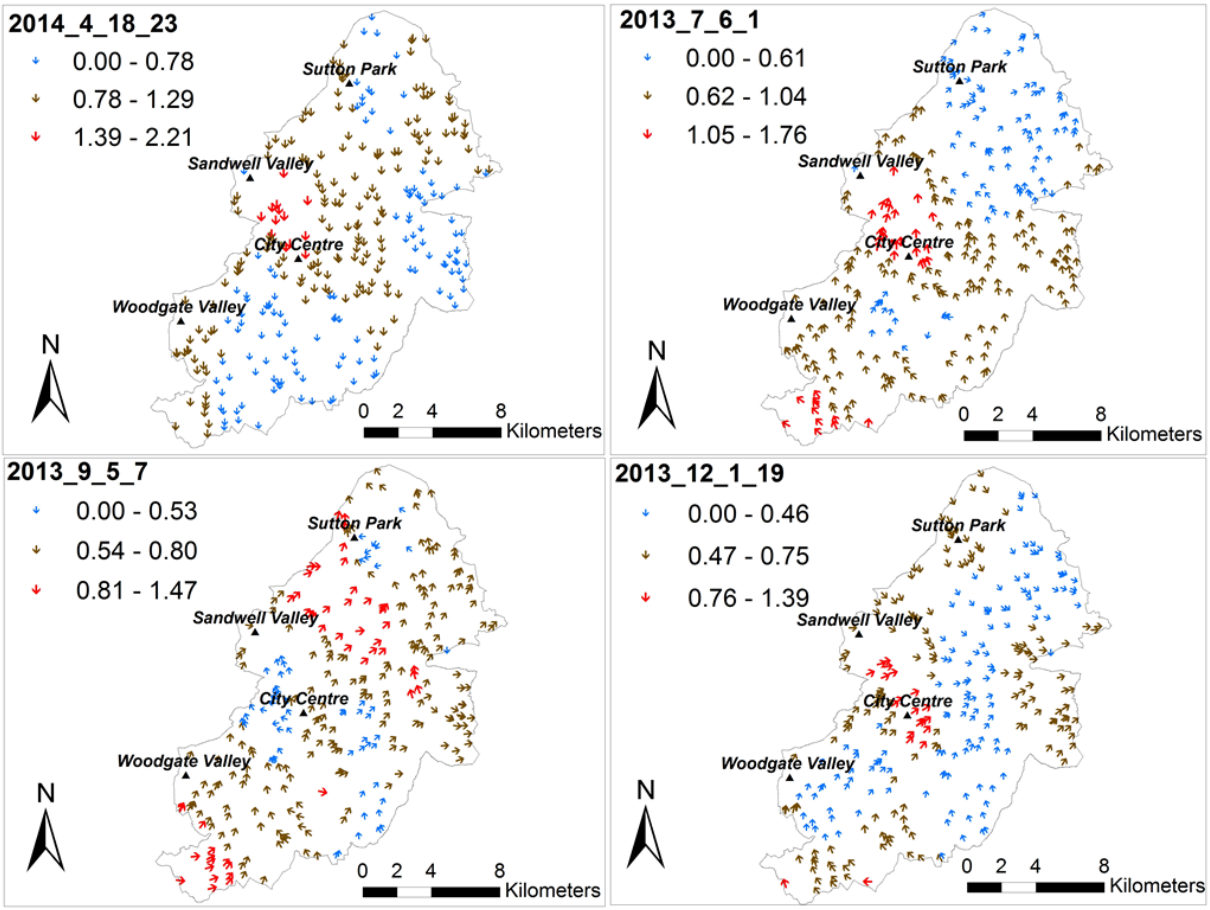

Fig.10 Seasonal wind speeds (m/s) and directions in Birmingham

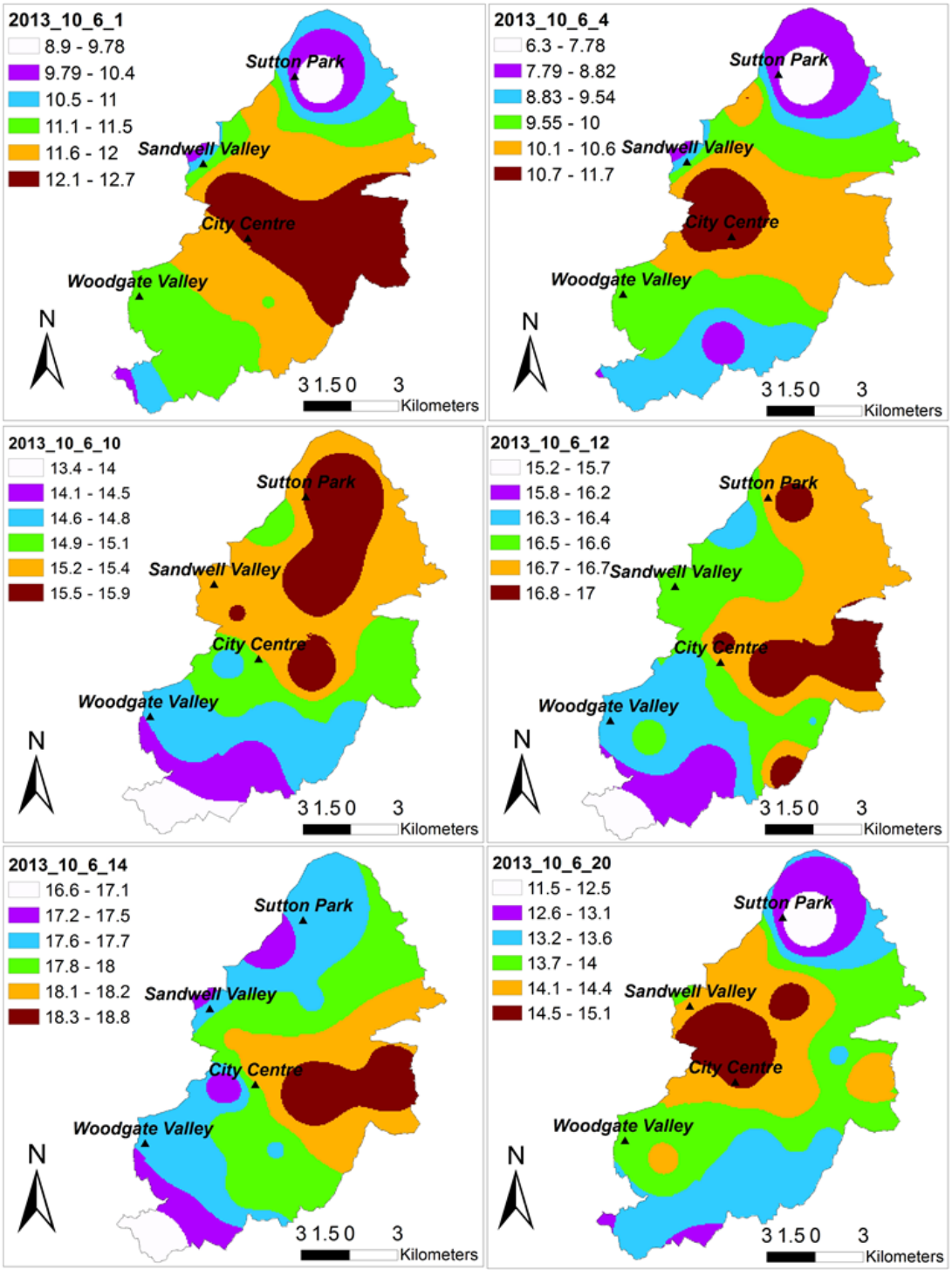

Fig.11 Daily UHI distribution in Birmingham (^{O}C)

C- Geometrical paramters derivation

The derivation of the geometrical parameters provided layers of sky view factor (SVF), visible sky (VS) and terrain view factor (TVF). The SVF and VS are dimensionless measures to estimate the visible area of the sky from an earth viewpoint [48], while, TVF is the opposite to them [49]. Fig.12 shows the variation SVF, VS and TVF through the entire city of Birmingham. Gal, et al. [50] have verified that the use of high resolution DEM as very useful to obtain a general picture of the geometrical size and shape of an urban environment.

The results showed that the SVF (0-1) and VS (1.9-100) values are low in the city centre and within dense trees areas but high in the open spaces. Conversely, the values of TVF are high in the city centre and low in the open spaces, due to the presence of high buildings in the city centre which do not exist in the open areas.

Pairs of stations close to each other have been chosen to investigate the impact of shadow patterns on air temperature. To be sure that no other functions are responsible for variations in temperature, it is necessary to compare stations that are close together, thus eliminating other variables. Another challenge is that the shadow is time dependant and varies significantly during the day. For these reasons, the effect of shadow on UHI formation has been investigated separately from other parameters. The hill-shade tool in ArcGIS creates a shaded relief from a surface raster by considering the illumination source angle and shadows [51]. The shadow areas can be distinguished by the black colour (Fig.13), and the areas of minimal or no shadows are scaled in shades of grey (1-254). The analysis of level of shadow did not show significant correlation with the air temperature. However, the presence of shade reduced the air temperature by up to 2 °C, by comparing the air temperature of a station in the shade and with one in no shade. Stations in Fig.13 a & b recorded lower temperatures when they are under shade compared to those exposed to the sunshine. Fig.13 c & d give examples when the shade moves from one station to another, and in both cases the station under the shade was slightly cooler than the one exposed to the sunshine. Moreover, all the pairs of stations in Fig.13 did not show significant variation of temperature measurements when they are under the shade or exposed to the sunshine at the same time. So the degree of illumination does not have a noticeable impact on the temperature's readings.

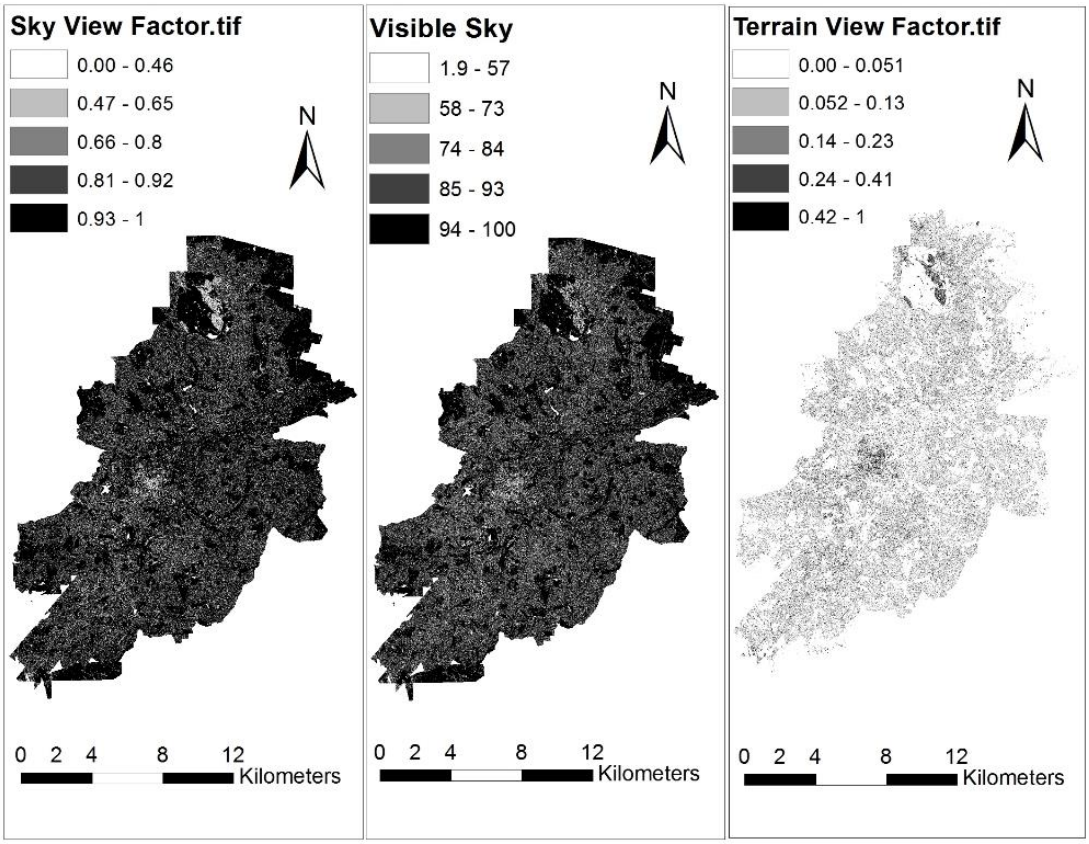

Fig. 9 Birmingham's SVF, VS and TVF (dimensionless)

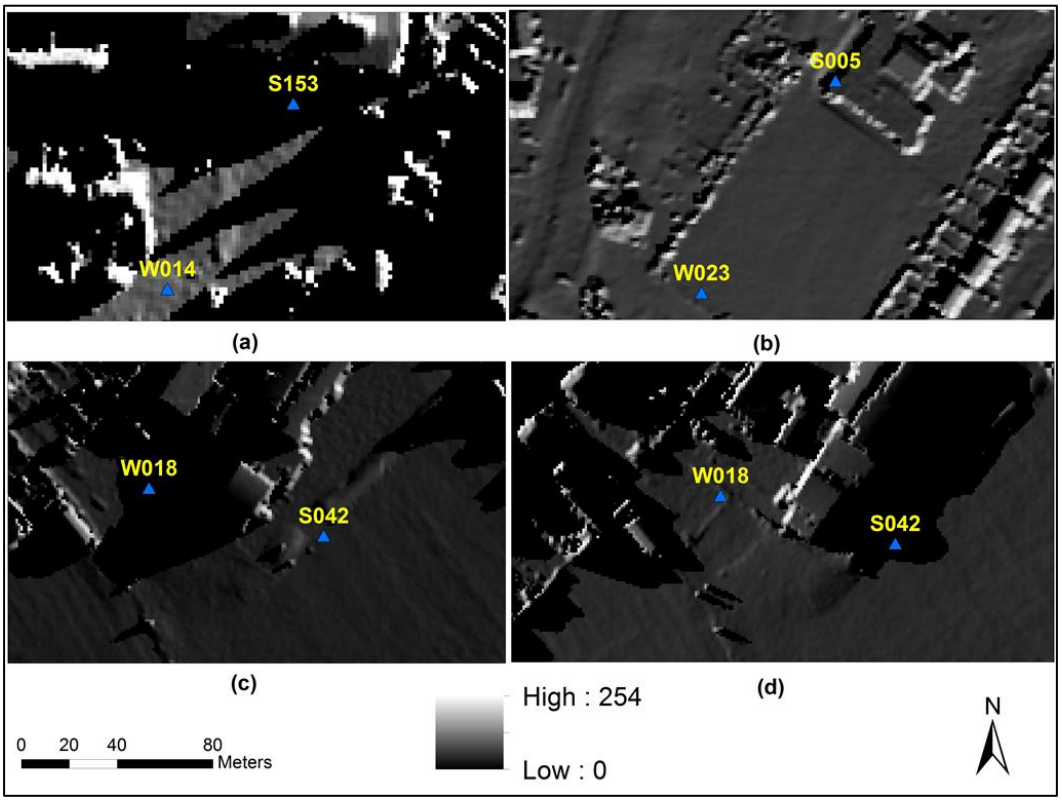

Fig.10 Shadow and illumination patterns for pairs of stations on the (a) 1st July 2013 at 6 am, (b) 30th November 2013 at 10 am, (c) 11th July 2013 at 5 am, and (d) 11th July 2013 at 7 pm.

D- Identifying influencing parameters

The modelling of the relationship between air temperature and influencing parameters was undertaken using multiple linear regressions by backward elimination of non-significant parameters. The air temperature was regressed against the land cover, land use and geometrical parameters at different times during the day and night. Days with high UHI intensity were chosen, and only highly significant p-values (<0.01) parameters were considered. 7113 observations were input to the regression models that cover the entire city of Birmingham. Table 3 and Table 4 show a sample output of the significant parameters on the UHI formation, and the summary statistics for the regression during night-time is detailed. The regression models in Table 3 and Table 4 have R Square 0.7 and 0.57 respectively, and the significant parameters were DTM, DSM, land class, urban atlas, topographic group, VS and TVF. In other words, the elevation, buildings' height, land cover, land use and geometrical parameters can influence up to 70% of the UHI.

Table 3 UHI influencing parameters on 1 July 2013 at 0 am

Date and time	**2013_7_1_0**	***Parameter***	***Coefficients (dimensionless)***
Regression Statistics		Intercept	15.711
		DTM	-0.010
Multiple R	0.8	DSM	-0.003
R Square	0.7	Land class	0.012
Adjusted R Square	0.7	Urban Atlas	-0.005
Standard Error	0.2	VS	0.001

Table 4 UHI influencing parameters on 1 July 2013 at 3am

Date and time	2013_7_1_3	*Parameter*	*Coefficients (dimensionless)*
Regression Statistics		Intercept	14.696
		TVF	-0.137
Multiple R	0.8	Topo. group	-0.005
R Square	0.6	DTM	-0.011
Adjusted R Square	0.6	DSM	-0.003
Standard Error	0.3	Urban Atlas	-0.004

Furthermore, the regression was applied on the hourly data of air temperature, and the significant relationships have been found to be coincided with high intensity UHI. Table 5 and Table 6 demonstrate the significant models during the day; the weather in the early morning at 6 am was scattered clouds and at 2pm mostly cloudy [36]. This clarifies the presence of UHI during the day as the clouds prevent the sunshine from reaching the ground. In this case the situation during the day will be similar to the night-time, and the only difference is the light which does not have noticeable impact of UHI, as proved earlier. Tables 5 and 6 demonstrate that the built up area (land class) contribute positively to the UHI intensity, and other parameters contribute negatively. This outcome agree with the results of Ryu and Baik [52] study that in the daytime the impervious surfaces contribute positively to the UHI, and the 3D urban geometry contributes negatively. It can be seen that the influencing parameters do not have the same influence during the day and night time. So, some parameters have shown to have notable impact during the night such as TVF, which does not have significant influence during the day time.

In general, it has been shown that land cover; land use and geometrical parameters influence the day and night UHI intensity, and can influence up to 70% of its effect. Moreover, the climatic condition can make the daytime UHIs resemble the night-time ones, but the influencing parameters may not be the same.

Table 5 UHI influencing parameters on 1 July 2013 at 6am

Date and time	2013_7_1_6	*Parameter*	Coefficients *(dimensionless)*
Regression Statistics		Intercept	12.914
Multiple R	0.8	Land class	0.030
R Square	0.7	DTM	-0.007
Adjusted R Square	0.7	DSM	-0.002
Standard Error	0.2	Urban Atlas	-0.003

Table 6 UHI influencing parameters on 1 July 2013 at 2pm

Date and time	2013_7_1_14	*Parameter*	*Coefficients (dimensionless)*
Regression Statistics		Intercept	17.000
Multiple R	0.64	DTM	-0.009
R Square	0.41	Land class	0.056
Adjusted R Square	0.41	Urban Atlas	-0.003
Standard Error	0.31		

4- Conclusions and recommendations

The use of HiTemp data has improved the spatiotemporal modelling of UHI, with its high densely network of sensors enabled producing of high spatial and temporal resolution images of UHI. Furthermore, the height of the stations provided information on the canopy layer under the level of buildings close to the energy sources. It was

found that UHI occurs in all seasons, day and night based on the climate condition. However, the high intensity UHI happens during the clear and calm weather. The maximum UHI intensity in Birmingham during the period of study was 13.53 °C. The wind speed and direction have important impact on the spatial distribution of the hot spots, as well as the extent of the UHI. The UHI occurred in the suburban areas as well as the urban areas due to the presence of impervious surface and anthropogenic activities. The city centre showed the lowest values of SVF and VS due to high buildings, which provided the shade to reduce the air temperature by up to 2 °C. A number of parameters' layers enabled the regression analysis to pick up significant relationships. The regression modelling could explain up to 70% of the influencing parameters when laid under the components of land cover, land use, and geometrical factors. Land class contributed positively to the UHI formation, but most land cover types and geometrical parameters had negative correlation with UHI. More data is needed such as classified urban materials and higher resolution meteorological data not captured by HiTemp such as soil moisture. Future work will investigate the impact of radiation fluxes on the UHI intensity.

Acknowledgements

The study was funded by the Iraqi government through its cultural attaché in London. This paper was supported by The Natural Environment Research Council (NERC) through providing HiTemp project's data. Also, the authors would like to thank The Birmingham Urban Climate Laboratory (BUCL) team as they were responsible for capturing the HiTemp data and provided useful explanations about some details. Furthermore, valuable data has been obtained from the Ordnance Survey and Met office, so their free of charge data was important to undertake this research.

References

[1] BUCL. (2014, 20 Augest 2014). *HiTemp Project*. Available: http://www.birmingham.ac.uk/schools/gees/centres/bucl/hitemp/index.aspx

[2] L. Gartland, *Heat Islands: understanding and mitigating heat in urban areas*. UK & USA: Earthscan, 2008.

[3] H. Radhi, F. Fikry, and S. Sharples, "Impacts of urbanisation on the thermal behaviour of new built up environments: A scoping study of the urban heat island in Bahrain," *Landscape and Urban Planning,* vol. 113, pp. 47-61, 5// 2013.

[4] Q. Weng, "Remote sensing of impervious surfaces in the urban areas: Requirements, methods, and trends," *Remote Sensing of Environment,* vol. 117, pp. 34-49, 2/15/ 2012.

[5] R. B. Balling, SW, "High-resolution surface-temperature patterns in a complex urban terrain," *Photographic Engineering Remote Sensing,* vol. 54, pp. 1289– 1293, 1988.

[6] J. E. Cermak, A. G. Davenport, E. J. Plate, and D. X. Viegas, "Wind climate in cities," 1995.

[7] J. A. Voogt and T. R. Oke, "Effects of urban surface geometry on remotely-sensed surface temperature," *International Journal of Remote Sensing,* vol. 19, pp. 895-920, 1998/01/01 1998.

[8] J. Wang, B. Huang, D. Fu, and P. M. Atkinson, "Spatiotemporal variation in surface urban heat island intensity and associated determinants across major Chinese cities," *Remote Sensing,* vol. 7, pp. 3670-3689, 2015.

[9] P. A. Mirzaei and F. Haghighat, "Approaches to study Urban Heat Island – Abilities and limitations," *Building and Environment,* vol. 45, pp. 2192-2201, 10// 2010.

[10] EPA. (2008, 1 June 2014). *Reducing Urban Heat Islands: Compendium of Strategies*. Available: http://www.epa.gov/heatisland/resources/pdf/BasicsCompendium.pdf

[11] EPA. (2013, 10 June 2014). *Heat Island Impacts*. Available: http://www.epa.gov/heatisland/impacts/index.htm

[12] P. A. Mirzaei, D. Olsthoorn, M. Torjan, and F. Haghighat, "Urban neighborhood characteristics influence on a building indoor environment," *Sustainable Cities and Society,* vol. 19, pp. 403-413, 12// 2015.

[13] D. J. Sailor, "Risks of summertime extreme thermal conditions in buildings as a result of climate change and exacerbation of urban heat islands," *Building and Environment,* vol. 78, pp. 81-88, 8// 2014.

[14] T. Berger, C. Amann, H. Formayer, A. Korjenic, B. Pospichal, C. Neururer, *et al.*, "Impacts of urban location and climate change upon energy demand of office buildings in Vienna, Austria," *Building and Environment,* vol. 81, pp. 258-269, 11// 2014.

[15] F. Busato, R. M. Lazzarin, and M. Noro, "Three years of study of the Urban Heat Island in Padua: Experimental results," *Sustainable Cities and Society,* vol. 10, pp. 251-258, 2// 2014.

[16] K. J. Doick, A. Peace, and T. R. Hutchings, "The role of one large greenspace in mitigating London's nocturnal urban heat island," *Sci Total Environ,* vol. 493, pp. 662-71, Sep 15 2014.

[17] D. Ivajnšič, M. Kaligarič, and I. Žiberna, "Geographically weighted regression of the urban heat island of a small city," *Applied Geography*, vol. 53, pp. 341-353, 9// 2014.
[18] P. Sismanidis, I. Keramitsoglou, and C. T. Kiranoudis, "A satellite-based system for continuous monitoring of Surface Urban Heat Islands," *Urban Climate*.
[19] Q. Weng and P. Fu, "Modeling annual parameters of clear-sky land surface temperature variations and evaluating the impact of cloud cover using time series of Landsat TIR data," *Remote Sensing of Environment*, vol. 140, pp. 267-278, 1// 2014.
[20] J. Rogan, M. Ziemer, D. Martin, S. Ratick, N. Cuba, and V. DeLauer, "The impact of tree cover loss on land surface temperature: A case study of central Massachusetts using Landsat Thematic Mapper thermal data," *Applied Geography*, vol. 45, pp. 49-57, 12// 2013.
[21] H. Zhang, Z.-f. Qi, X.-y. Ye, Y.-b. Cai, W.-c. Ma, and M.-n. Chen, "Analysis of land use/land cover change, population shift, and their effects on spatiotemporal patterns of urban heat islands in metropolitan Shanghai, China," *Applied Geography*, vol. 44, pp. 121-133, 10// 2013.
[22] H. C. Ho, A. Knudby, P. Sirovyak, Y. Xu, M. Hodul, and S. B. Henderson, "Mapping maximum urban air temperature on hot summer days," *Remote Sensing of Environment*, vol. 154, pp. 38-45, 11// 2014.
[23] L. Chapman, C. L. Muller, D. T. Young, E. L. Warren, C. Grimmond, X.-M. Cai, *et al.*, "The Birmingham Urban Climate Laboratory: An open meteorological testbed and challenges of the smart city," *Bulletin of the American Meteorological Society*.
[24] O. f. N. Statisics. (2015, 12-08-2015). *Anuual Mid-year Population Estimates, 2014*.
[25] C. J. Tomlinson, L. Chapman, J. E. Thornes, and C. J. Baker, "Derivation of Birmingham's summer surface urban heat island from MODIS satellite images," *International Journal of Climatology*, vol. 32, pp. 214-224, 2012.
[26] D. J. Unwin, "THE SYNOPTIC CLIMATOLOGY OF BIRMINGHAM'S URBAN HEAT ISLAND, 1965–74," *Weather*, vol. 35, pp. 43-50, 1980.
[27] D. B. Johnson, "Urban modification of diurnal temperature cycles in birmingham, U.K," *Journal of Climatology*, vol. 5, pp. 221-225, 1985.
[28] A. V. Bradley, L. Chapman, and J. E. Thornes, "Modelling of road surface temperature from a geographical parameter database. Part 2: Numerical," *Meteorological Applications*, vol. 8, pp. 421-436, 2001.
[29] O. S. (GB). (2015). *Topography [FileGeoDatabase geospatial data]*. Available: http://digimap.edina.ac.uk
[30] EDINA. (2015, 15/5/2015). *Digimap: Data download, OS Terrian 5 DTM*. Available: www.digimap.edina.ac.uk/datadownlaod/osdownlaod
[31] EEA. (2014, 18 Sep. 2015). *Urban Atlas*. Available: www.eea.europa.eu/data-and-maps/data/
[32] S. M. Owen, A. R. MacKenzie, R. G. H. Bunce, H. E. Stewart, R. G. Donovan, G. Stark, *et al.*, "Urban land classification and its uncertainties using principal component and cluster analyses: A case study for the UK West Midlands," *Landscape and Urban Planning*, vol. 78, pp. 311-321, 11/28/ 2006.
[33] OS. (2014, 23 Feb. 2014). *Research At Ordnance Survey*. Available: www.ordnancesurvey.co.uk/eduaction-research/research/index.html
[34] Esri. (2015, 20/10/2015). *Basemaps*. Available: http://www.esri.com/data/basemaps
[35] Geomatics. (2014). *LIDAR* Available: https://www.geomatics-group.co.uk/GeoCMS/Products/LIDAR.aspx
[36] M. Office. (26/6/2015). *MIDAS*. Available: www.catalogue.eda.ac.uk/uuid/220a65615218d5c9cc9e4785a3234bd0
[37] Z. Xu and V. Coors, "Combining system dynamics model, GIS and 3D visualization in sustainability assessment of urban residential development," *Building and Environment*, vol. 47, pp. 272-287, 1// 2012.
[38] P. P.-Y. Wong, P.-C. Lai, C.-T. Low, S. Chen, and M. Hart, "The impact of environmental and human factors on urban heat and microclimate variability," *Building and Environment*, vol. 95, pp. 199-208, 1// 2016.
[39] S. Kardinal Jusuf, N. H. Wong, E. Hagen, R. Anggoro, and Y. Hong, "The influence of land use on the urban heat island in Singapore," *Habitat International*, vol. 31, pp. 232-242, 6// 2007.
[40] N. R. S. Draper, H, *Applied regression analysis*
New York: Wiley, 1998.
[41] G. E. Dallal. (2000, 15/1/2016). *P Values*. Available: http://www.jerrydallal.com/lhsp/pval.htm
[42] T. a. Date. (2013, 12/8/2015). *Sun in Birmingham*. Available: www.timeanddate.com/sun/uk/birmingham?mont=9&year=2013
[43] M. Alcoforado and H. Andrade, "Global Warming and the Urban Heat Island," in *Urban Ecology*, J. Marzluff, E. Shulenberger, W. Endlicher, M. Alberti, G. Bradley, C. Ryan, *et al.*, Eds., ed: Springer US, 2008, pp. 249-262.
[44] M. office. (2015, 29/7/2015). *July 2013 heat wave*. Available: www.metoffice.gov.uk/learning/learn-about-the-weather/weather-phenomena/case-studies/heat-wave-july2013
[45] M. Office. (2016, 25-5-2016). *Beaufort wind force scale*. Available: http://www.metoffice.gov.uk/guide/weather/marine/beaufort-scale
[46] M. Roth, "Urban Heat Islands," in *Handbook of Environmental Fluid Dynamics, Volume Two*, ed: CRC Press, 2012, pp. 143-160.

[47] T. R. Oke, "Boundary layer climates (Second edition). By T. R. Oke. Methuen. 1987. Pp. 435 + xvi. £39.95 hardback; £14.95 paperback," *Quarterly Journal of the Royal Meteorological Society*, vol. 114, pp. 1568-1568, 1988.
[48] D. S. R. a. J. F. G. M. Léa C.L.Souza, "SKY VIEW FACTORS ESTIMATION USING A 3D-GIS EXTENSION," presented at the Eighth International IBPSA Conference Eindhoven, Netherlands 2003.
[49] J. Böhner and O. Antonić, "Chapter 8 Land-Surface Parameters Specific to Topo-Climatology," in *Developments in Soil Science*. vol. Volume 33, H. Tomislav and I. R. Hannes, Eds., ed: Elsevier, 2009, pp. 195-226.
[50] T. Gal, F. Lindberg, and J. Unger, "Computing continuous sky view factors using 3D urban raster and vector databases: comparison and application to urban climate," *Theoretical and applied climatology*, vol. 95, pp. 111-123, 2009.
[51] A. R. Center. (2011, 20/8/2015). *Hillshade*. Available: www.help.arcgis.com/en/arcgisdesktop/10.0/help
[52] Y.-H. Ryu and J.-J. Baik, "Quantitative Analysis of Factors Contributing to Urban Heat Island Intensity," *Journal of Applied Meteorology and Climatology*, vol. 51, pp. 842-854, 2012/05/01 2012.